Underdamped commensurate dynamics in a driven Frenkel-Kontorova–type model

A. Vanossi,[1,2] J. Röder,[1] A. R. Bishop,[1] and V. Bortolani[2]
[1]*Theoretical Division and Center for Nonlinear Studies, Los Alamos National Laboratory, Los Alamos, New Mexico 87545*
[2]*INFM-S3 e Dipartimento di Fisica, Università di Modena e Reggio Emilia, Via Campi 213/A, 41100 Modena, Italy*
(Received 13 June 2002; published 15 January 2003)

The dynamics of a Frenkel-Kontorova chain subject to a substrate potential with a *multiple-well* structure and driven by an external dc force is studied in the *underdamped regime*. Making a *rational* choice among the three inherent length scales characterizing the system allows us to consider the possible formation of commensurate structures during sliding over the complex on-site potential. We comment both on the nature of the particle dynamics in the vicinity of the pinning-depinning transition point, and on the dynamical states displayed during the chain motion at different strengths of the dc driving. Varying the number of particles in the simulations allows us to consider, on a multiple-well substrate, the role played by the *coverage variable* on the depinning mechanism. The dependence of the minimal force required to initiate the chain motion (*static friction*) on the ratio of the model interaction strengths is analyzed and compared to the well-known case of the standard Frenkel-Kontorova model, which has only two inherent lengths.

DOI: 10.1103/PhysRevE.67.016605 PACS number(s): 05.45.−a, 45.05.+x, 64.70.Rh, 63.20.Pw

I. INTRODUCTION

More than 60 years ago, Frenkel and Kontorova used a simple discrete one-dimensional (1D) model, first analytically treated by Dehlinger [1], to describe the dislocation dynamics in crystals [2]. This model has nowadays become very popular in many branches of solid state and nonlinear physics [3]: domain walls in ferroelectrics, the problem of crowdions localized interstitial defects in a metal, superionic conductors, submonolayer films of atoms on crystal surfaces, surface reconstruction phenomena, DNA dynamics and denaturation, the theory of Josephson junctions, and so on. Especially in connection with solid friction phenomena, the application of *driven* Frenkel-Kontorova (FK) type models has recently received an increasing interest [4] as a possible interpretative tool to more deeply understand the complex field of *nanotribology*, i.e., of the atomic processes occurring at the nanoscale between the interfaces of interacting materials in relative motion. In these one-dimensional models, a certain density of interacting particles is made to slide, in the presence of dissipation, over a rigid substrate potential by the application of an external (impulsive, dc or ac) driving force. These modeling studies have been mainly stimulated by the microscopic approaches, both experimental and computational, developed during the past few years for the theory of friction. Indeed, recent advances in technology [5], notably the use of the atomic-force microscope, the friction-force microscope, surface-force apparatus, and the quartz-crystal microbalance, have provided the possibility to build experimental devices able to perform well-defined analyses on well-characterized materials at the nanoscale. Simultaneously, the evolution of powerful computers now allows microscopic investigations (e.g., molecular dynamics simulations with realistic potentials [6]) able to supply very detailed information on the atomic scale for realistic sliding systems. Such simulations can, however, become extremely demanding, particularly when three-dimensional calculations are performed. This recent acceleration in the acquisition of experimental and computational data has brought searches for simple mathematical models capable of describing, in a more immediate and understandable way, the essential physics involved in tribological phenomena.

In its simplest form, the *standard* FK model, whose systematic and analytical study is mainly due to Aubry's work [7], consists of a one-dimensional chain of particles coupled by a *harmonic* nearest-neighbor interaction under the influence of an external spatially periodic (*sinusoidal*) potential. The essential physical feature of the model consists of the competition between these two types of interactions: the former favors a uniform separation among particles; the latter tends to pin the atom positions to the bottom of the substrate wells. This competition, often referred to as *frustration* or, more specifically, *length scale competition*, results in a rich complexity of spatially modulated structures.

Some important generalizations of the FK model have already been taken into account by studying more general types of substrate potential, as well as anharmonic interactions in the chain. As far as the on-site potential is concerned, its introduction can be justified [8] via a self-consistent microscopic model where only interparticle interaction is considered. The on-site substrate potential in the FK model can, in fact, be viewed as an effective potential produced by the coupling of the chain atoms with other degrees of freedom such as, the substrate atoms. Moreover, the simple sinusoidal potential corresponds to the lowest possible approximation. Namely, when the substrate particles constitute a simple lattice with one atom per elementary cell, and where, in the Fourier expansion of the interaction potential, the main approximation is given by the first harmonic.

To model real physical systems, it is sometimes helpful to consider substrate potentials which may vary substantially from the regular one assumed in the standard FK model, with a possible consequent drastic change in the friction dynamics between the two solid interfaces. The deviation of the substrate potential from the sinusoidal shape changes the parameters of both linear and nonlinear interactions. This may lead to qualitatively different features such as the appearance of different types of kinks, phonon branches, changes in kink-

antikink collisions, and modification of breather (kink-antikink bound state) solutions. In general, at low external fields, the dynamics is governed by a mechanism that can be identified as the motion of kinklike structures. As the imposed driving is increased, a *nonlinear* evolution regime occurs. Then, for large external forces, the barriers to the particle motion are completely suppressed, and the ''current'' becomes proportional to the applied field. In the presence of substrate potentials with several different minima and maxima (and therefore also of possible different types of kink structures), we might, for example, expect some different behaviors in the chain mobility response at low-driving regimes.

In a recent work [9], the case of a driven one-dimensional array of particles sliding over a quasiperiodic substrate potential has been analyzed. This study, characterized by the absence of periodicity (the maxima and minima of the potential are no longer evenly spaced, nor are they of equal amplitudes), was motivated in order to gain insight into the more complex problem of friction between two disordered solids, by starting from this precisely defined case, intermediate between order and true randomness. The three inherent lengths of the system, two of which define the quasiperiodic substrate geometry and one of which characterizes the natural equilibrium separation among the chain particles, were chosen to be mutually *incommensurate* (i.e., each of the three length scales in the model was incommensurate with respect to the other two). This choice allowed the analysis of the dynamic behavior of an equivalent FK quasiperiodic system previously studied in the pure static regime [12]. Due to the geometrical features of this quasiperiodic system, it is theoretically possible to compare the numerical simulations with recent experimental results obtained in tribological studies between quasicrystalline solid surfaces [13]. However, in practice, it would probably first be necessary to generalize this model to at least two dimensions, where it would be possible for the sliding particles to avoid passing over the highest barriers in the substrate potential, which they have to overcome in one dimension. It should be noted also that the present experimental data on quasicrystal tribology does not clearly relate desirable frictional properties with unique atomic arrangements.

Given the recognized importance of the mathematical properties (*number theory*) of the different length scales involved in FK models [7], it is natural to recall that the absence of translational invariance (that an incommensurate choice of the substrate characteristic length scales would imply for a quasiperiodic function) does not signify a complete lack of order as, for example, in the case of true randomness. The ''regular features'' of this order are indeed restored in the framework of a general classification, familiar in crystallography, called *superspace group theory* [14], which proves how aperiodic, but not amorphous, structures can be embedded in a higher-dimensional space.

In this paper, we shall, instead, restrict ourselves to the case of *commensurate* choices among the three model length scales. This allows us to consider, in the underdamped dynamical regime, the possible formation of commensurate structures during the sliding of a one-dimensional FK chain over a complex substrate potential.

The paper is organized as follows. In the following section, we present the driven FK-type model subject to the complex, (*multiple-well*) substrate potential and to a weak viscous dissipative term. The numerical technique implemented to solve the equations of motion is summarized in Sec. III. Section IV is devoted to the obtained simulation results for different rational choices of the inherent model lengths. The pinning-depinning transition is studied as a function of the number of chain particles (*coverage variable*) and for different values of the interaction strengths. The commensurate structures emerging during the chain motion and characterizing the different dynamical states in the mobility curve are displayed. Conclusions are given in Sec. V.

II. MODEL

We consider the dynamics of a FK-type chain, whose N particle positions $\{x_i\}$ satisfy the following equations of motion:

$$\ddot{x}_i+\gamma\dot{x}_i+\frac{1}{2}\left\{\sin\frac{2\pi x_i}{a}+\sin\frac{2\pi\beta x_i}{a}\right\}+\frac{d}{dx_i}\left[\sum_{j\neq i}V(|x_i-x_j|)\right]=F, \tag{1}$$

where γ is a phenomenological viscous damping coefficient, chosen such that we are in the underdamped regime, and F is the external driving force; the coefficient γ can be thought of as representing degrees of freedom inherent in real, physical systems which are not explicitly included in our model (e.g., vibrational or electronic excitations in the substrate). Regarding this topic, a 2D isotropic elastic model has been recently introduced [10] to study the flow of energy away from a sliding interface between two atomistically flat workpieces. This model does not include any extrinsic damping terms, thus allowing an isolated examination of the way, in which the propagation of energy away from the sliding interface affects the friction process. At least qualitatively, the behavior observed was similar to that seen in simple 1D friction models including *ad hoc* viscous damping [11]. This result provides indirect evidence that the effects of the degrees of freedom eliminated in simple models on the remaining degrees of freedom can be approximated by the inclusion of a viscosity term in the equations of motion. In Eqs. (1), the interatomic interaction is chosen to be of the simple harmonic form

$$V=\frac{K}{2}(x_{i+1}-x_i-b)^2, \tag{2}$$

with a strength K and a natural equilibrium spacing b determined by the ratio L/N, where L is the chain length. The two lengths defining the on-site substrate potential are then a and $c=a/\beta$. In the limit that $\beta=1$, the model contains only two length scales and we retrieve the standard FK model.

As already stated, in the present work, these characteristic lengths are chosen to be mutually commensurate, i.e., $a/c=M_1/M_2$, with M_1 and M_2 integer numbers. This means that the periodicity T of the substrate turns out to be T

$=M_2a=M_1c$. Here, we will fix $a=1$ and vary the parameter β. Naturally, imposing periodic boundary conditions on the system, implies that the chain length L must be an integer multiple Q of the period T.

III. NUMERICAL PROCEDURE

The following scheme to vary adiabatically the driving force was implemented in a fourth-order Runge-Kutta algorithm to solve numerically the equations of motion (1). The system was initialized with the particles placed at rest at a uniform separation b. The dc force F was then increased adiabatically from 0 to 1 in steps $dF=0.005$. For every value of F, and with a sufficiently small time step ($dt=0.006$), Eqs. (1) were integrated over a time period ($t=300$), which was long enough to eliminate transient behavior and reach a steady state. The average system velocity

$$\langle v\rangle=\frac{1}{N(t_f-t_i)}\int_{t_i}^{t_f}\sum_{i=1}^{N}\dot{x}_i dt \tag{3}$$

was then calculated over a time $t_f-t_i=150$. The final chain configuration (positions and velocities) obtained at one value of F was used as the initial condition for the integration of the dynamics for the next value of the driving.

IV. RESULTS

Our numerical simulations have shown that the different dynamical structures emerging during the motion of the chain particles over the substrate potential must possess, due to the existence of periodic constraints and of the substrate periodicity T, commensurate lengths. Explicitly, all the possible periodicities for these dynamical particle configurations in the chain are given by the factors of QT. Moreover, when these structures moving around the chain have a commensurate length larger than the substrate period, their topological shape often turns out to be decorated (depending also on the ''commensurability'' of the number of particles N with respect to the substrate characteristic lengths) by superimposed smaller deformable particle configurations respecting the same periodicity T of the on-site potential. Naturally, the possibility to display, during the dynamics, a variety of different length structures is constrained by the chain stiffness, i.e., the value of the interatomic strength K, as well as by the number of chain particles N, due to the imposed periodic boundary conditions $TQ=bN(=L)$.

In the following, restricting ourselves to commensurate ratios of the characteristic lengths of the model, we shall analyze the behavior of the chain motion for a finite system size L, commenting both on the nature of the particle dynamics in the vicinity of the pinning-depinning transition, and on the dynamical states displayed during the particle motion at different values of the driving, F. The dependence of the minimal value of the force, F_s required to initiate the chain motion (*static friction*) on the ratio of the interparticle and substrate interactions will be considered and compared to the standard FK model.

Chain length L. The substrate periodicity T is contained

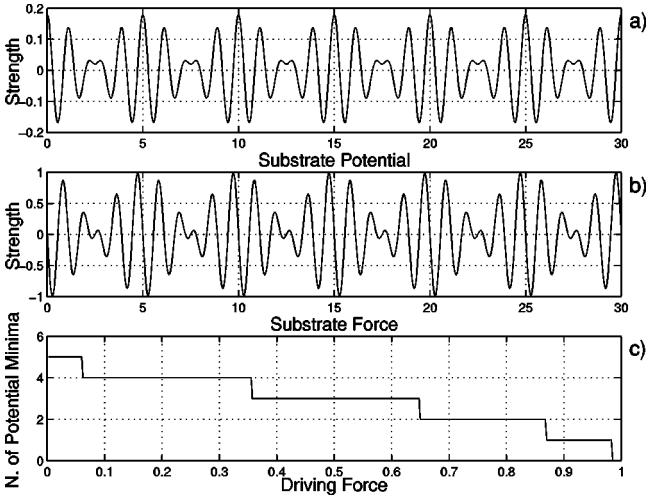

FIG. 1. Substrate potential and force for $\beta=24/30$. The bottom subplot shows the progressive disappearence of the five potential minima vs the driving force due to the substrate tilting.

an integer number of times in the system length L for values of $\beta=M_1/L$, with $M_1=1,\ldots,L$. In principle, we have, therefore, the possibility of simulating the dynamics of the chain particles over L different substrate potentials. From Eqs. (1), for $M_1=L$, the standard driven FK model is recovered. Due to the impossibility, for every fixed value of L, of studying the chain dynamics for each specific substrate shape in detail, we will consider just a few examples, in an attempt to give a general idea of the characteristic system behavior. Additionally, varying the number of chain particles allows us to analyze on a complex substrate, with different spacings and amplitudes among its maxima and minima, the role played by the *coverage variable* (defined as the ratio of the number N of atoms to the number of minima in the substrate potential) on the depinning mechanism.

We now consider some specific values of the parameter β allowed by the imposed periodic boundary conditions for a system of length L.

1. $\beta=24/30$ $(L=30,M=24)$

Figures 1(a) and 1(b) show, respectively, the substrate potential and substrate force for the system size $L=30$ for the chosen values of the model parameters. In each substrate unit cell of period $T(=5)$, we count five wells for the $\beta=24/30$ case. The effect of the external driving, F, is to tilt the potential, producing a corrugated surface whose average slope is determined by F. Increasing the driving leads, in the presence of a *complex* substrate, to a *sequential* disappearance of the potential minima [see Fig. 1(c)] until the situation with no stable positions for the chain particles is reached.

For an undriven analysis ($F=0$), the most commensurate case is obtained by placing 30 particles in the system size $L=30$, so that we have one particle per well. However, from a dynamical point of view, we notice that once we tilt the on-site potential by the application of the external force, the lowest minima, having a height much smaller than the others, soon disappear and each substrate cell then contains only

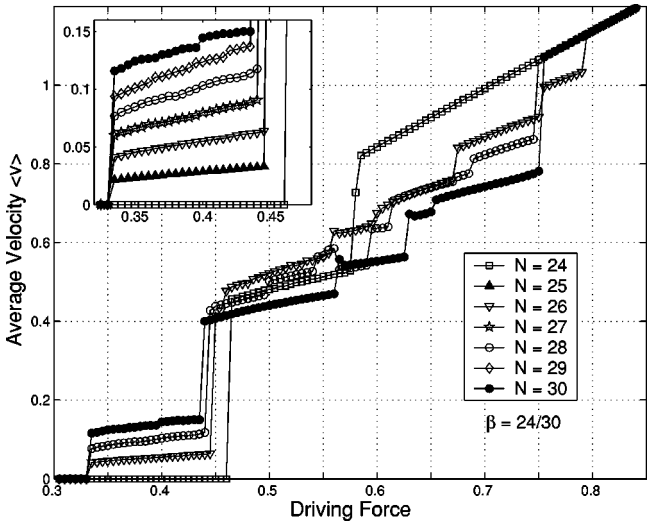

FIG. 2. Average mean chain velocity vs driving. Systems with different numbers N of particles are shown. Specifically, the inset shows, near the depinning transition, the proportionality of $\langle v \rangle$ to the particle number. Other parameters are $K=1$ (harmonic interaction) and $\gamma=0.7$ (underdamped regime).

four wells. Hence, *dynamically* the case $N=24$ is the most ''commensurate.''

Figure 2 represents the average mean chain velocity, as a function of the driving F, for chains with different numbers N of particles. As far as the pinning-depinning transition is concerned, we can observe that for $N=24$, there are no extra particles (kinks) in place to initiate the motion when the Peierls-Nabarro (PN) barrier disappears. Consequently, without any noise or thermal fluctuations to create a kink, the chain motion does not start when we exceed the PN barrier and dynamics is delayed. Then, as the number of particles $N=25,26,\ldots$, etc., is increased, each extra particle provides one more ''intrinsic'' kink, and the pinning-depinning transition occurs at a lower value of the driving (compared to the case with $N=24$), i.e., as soon as the PN barrier is exceeded.

We observe a rise in the mobility that is roughly proportional to the number of these *intrinsic* kinks, up until $N=30$ (see inset of Fig. 2). For the same value of the external driving ($F=0.375$), just above the depinning transition, four particle trajectory configurations are shown in the subplots of Fig. 3. As can be observed, each added particle above $N=24$, corresponds to an extra kink propagating through the chain. An approximate evaluation of the PN barrier, obtained by placing four particles per cell, adding one more particle and forcing the extra particle to move from one cell to the next, whilst minimizing the energy of the system for each position of this extra particle, gives good agreement between the point, at which there is no barrier for the kink to move and the point, at which motion begins in the simulations.

Because of the more complex substrate potential as compared to the simple sinusoidal one of the standard driven FK model, it is not easy to trace a precise relation between the steps shown in the curves of the averaged chain velocity versus the external driving force, above the depinning threshold, and the various dynamical behaviors observed during

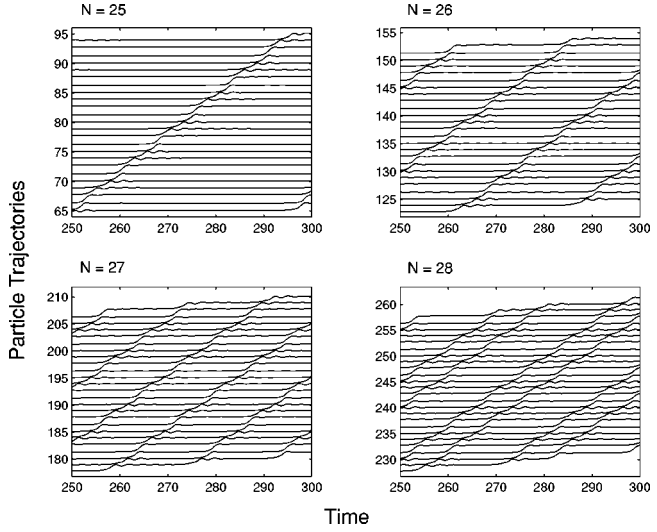

FIG. 3. Particle trajectories for chains with a different number of extra atoms, slightly above the depinning transition ($F=0.375$). Other parameters are as in Fig. 2.

the chain motion. Moreover, these regimes, characterized by rearrangements of particle configurations (spatial inhomogeneities) and by different periodicities and amplitudes of the structures moving around the chain, turn out to be strongly dependent also on the number of system particles and on the chain stiffness.

For the choice of the parameter $\beta=24/30$ and a chain composed of 30 particles, the dynamics exhibits, for different values of the driving F, commensurate structures, as shown in Fig. 4. The periodicities of these structures turn out to be 5, 10, 15, and 30: these are all the possible values that are both multiples of the substrate periodicity $T=5$ and factors of the length, $L=30$. The corresponding particle trajectories, all displayed for the same time interval, are presented in the four insets of Fig. 5. In this picture, it is not important to figure out all the details for each particle trajectory; the reader, instead, should notice the presence of the visible dark

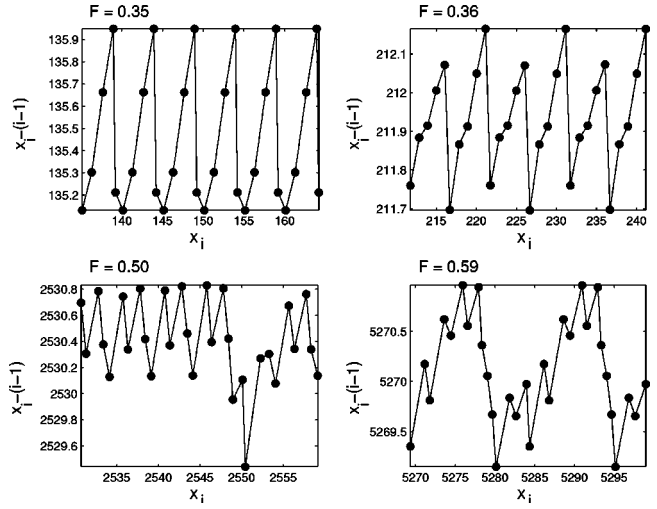

FIG. 4. Commensurate structures of different periodicities in the dynamics of a 30-particle chain for four values of the force F.

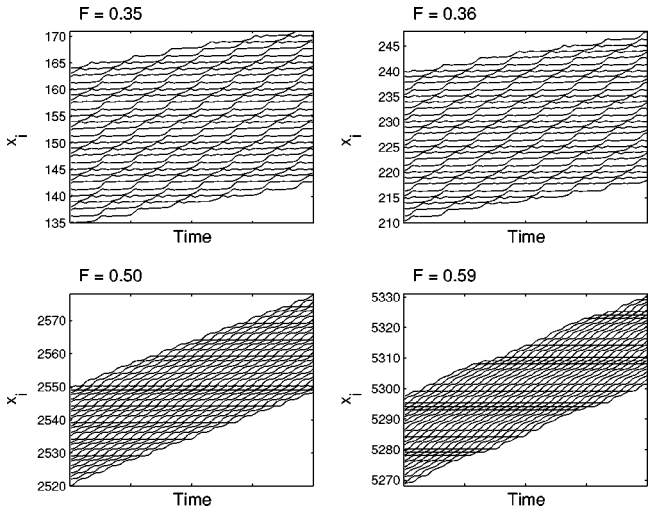

FIG. 5. Particle trajectories vs time corresponding to the four commensurate structures shown in the insets of Fig. 4.

(localized chain compressions) and light (localized chain expansions) ''stripes'' corresponding to the commensurate structures displayed, previously, in Fig. 4.

These dynamical structures moving around the chain often show superimposed decorations of period T. The fact that in this case, these decorations of length 5 are each formed by five particles is merely due to the number $N=30$ of particles constituting the chain. For a chain with $N=24$ and for the same value of β, the simulations revealed that the structures exhibiting a characteristic length of period $T=5$ are, in fact, made up of four particles.

It is reasonable to expect that increasing the system stiffness, i.e., the value of the interatomic strength K, will reduce the possible periodicities of the moving structures since the relative separations of the chain particles will be much more constrained. Consequently, as shown in Fig. 6, spatially inhomogeneous intermediate states, between the locked con-

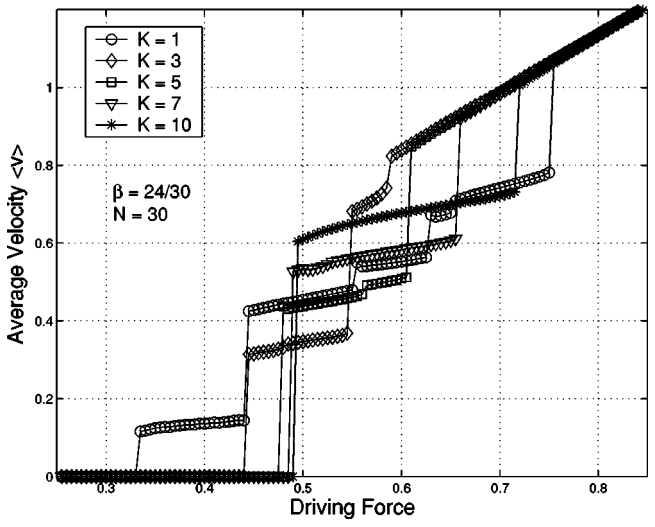

FIG. 6. Average mean chain velocity vs driving for different values of the interatomic strength K. Other parameters are as shown.

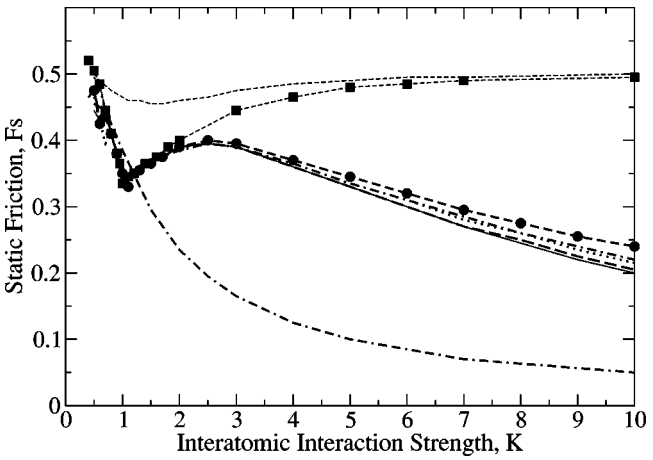

FIG. 7. Static friction F_s, vs interatomic interaction strength K, for $\beta=24/30$. The results are plotted for various numbers of chain particles: $N=18$ (dash-dash-dotted line), $N=24$ (dashed line), $N=25$ (solid line), $N=26$ (long-dashed line), $N=27$ (long-dashed line with circles), $N=28$ (dot-dashed line), $N=29$ (dotted line), and $N=30$ (dashed line with squares).

figuration and the running one, tend to decrease in number for increasing values of K.

We have also investigated the dependence of the static friction F_s on the interatomic interaction strength K for various numbers of particles, N. Some of the results are shown in Fig. 7.

Although the exact forms of the curves are complicated and different for each number of particles, (and also for each value of β), one notices that the curves can be separated into two groups, depending on their limit for large K. The plots for $N=24$ and 30 particles approach the value 1/2, whereas the other cases plotted tend to zero, as K increases. There is a third possibility not shown on Fig. 7. For only six particles in the chain, the static friction is 1, independent of the interatomic interaction. To see how these three categories arise, consider the possible *stable* particle configurations when the chain is pinned. These must satisfy the equations

$$\frac{1}{2}(\sin 2\pi x_i+\sin 2\pi\beta x_i)+K(x_{i+1}+x_{i-1}-2x_i)=F. \tag{4}$$

So, summing over all particles in the chain we obtain

$$\sum_{i=1}^{N}(\sin 2\pi x_i+\sin 2\pi\beta x_i)=2NF. \tag{5}$$

For $K\gg 1$, the particles are nearly equally separated, i.e., $x_i=iL/N+\Delta+O(1/K)$, where Δ is a uniform shift for all particles. Substituting this into Eq. (5) and noting that $\beta=M/L$ we see that

$$\sum_{i=1}^{N} \sin\left(\frac{2\pi Li}{N}\right)\cos(2\pi\Delta)+\cos\left(\frac{2\pi Li}{N}\right)\sin(2\pi\Delta)$$
$$+\sin\left(\frac{2\pi Mi}{N}\right)\cos(2\pi\beta\Delta)+\cos\left(\frac{2\pi Mi}{N}\right)\cos(2\pi\beta\Delta)$$
$$=2NF. \quad (6)$$

For most choices of parameters, the sums above will add to zero. So, there is no possible stable solution for $F>0$ and the static friction will vanish as $K\to\infty$. However,whenever N is a factor of M or L, then the summations will not vanish and a nonzero static friction will result. The static friction will then be, either 0.5, if N is a factor of either M or L (the cases $N=24,30$ shown in Fig. 7), or 1, if N is a factor of both M and L ($N=6$ for $\beta=24/30$ and $L=30$).

One notable feature of the curves is that they can be *nonmonotonic*. This is in contrast to the normal FK model, where one obtains a constant static friction with one particle per potential well, and a static friction that decreases with K when an extra particle is present. A study of the pinned configurations in our model shows that a restructuring occurs in the stable state of the cells with six particles at the value $K=1$. This leads to the characteristic downward spike in the static friction at $K=1$ when $N=25$, 26, 27, 28, 29, and 30. Similar changes in the pinned states as one varies the elastic constant K, have been observed in other studies and have also produced unusual features in the behavior of the static friction [9]. It is the complex, multiple-well nature of the substrate potential that allows for a discontinuous change in the stable positions of the particles as one varies the elastic constant, and so permits the nonmonotonic behavior.

2. $\beta=32/40$ ($L=40, M=32$)

We have verified that similar results are obtained considering the depinning mechanism of a chain with a different length L and the same value of the parameter β, so that the substrate is characterized by the same shape and periodicity $T(=5)$ as above. In this case the dynamics are again delayed when no intrinsic kinks are present in the chain (for $N=32$) and the mobility increases, just above the pinning-depinning transition point, proportionally to the number of these intrinsic kinks (from $N=33$ to $N=40$), until there is one extra atom per periodic cell.

3. $\beta=25/30$ ($L=30, M=25$)

Essentially the same observations are possible for the potential displayed in Fig. 8, in which a very small potential maximum divides two adjacent minima. Its rapid disappearance upon application of the external driving leaves the five cells contained in the system size $L=30$ with five wells each.

The averaged mean chain velocity shown in Fig. 9 emphasizes that, dynamically, the most commensurate case, where no intrinsic kinks are present to initiate the motion, is the one corresponding to $N=25$.

4. Other ratios

We have also carried out simulations for other rational choices of the inherent lengths defining the model and allowed by imposing periodic boundary conditions on a finite system of size L. For all these simulations, we have recovered dynamical behavior consistent with the previously mentioned observations regarding the system commensurability.

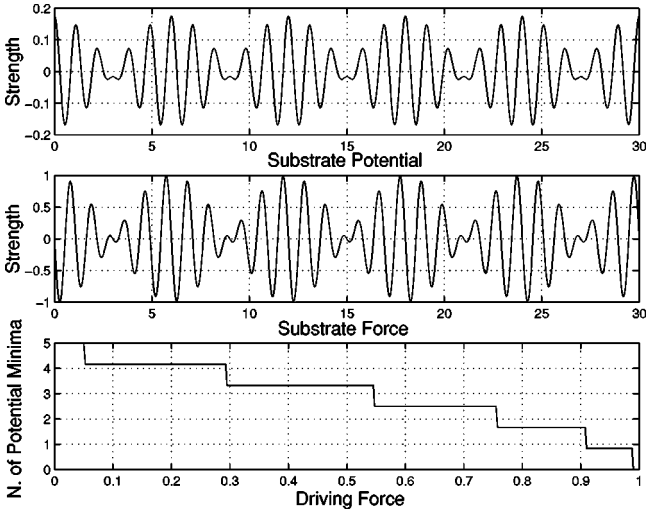

FIG. 8. Substrate potential and force $\beta=25/30$. The bottom subplot shows the progressive disappearence of the five potential minima vs the driving force due to the substrate tilting.

V. CONCLUSIONS

In this paper, we have studied the dynamics of an interacting chain of atoms driven, over a *complex* (yet periodic) substrate potential, by a dc external force and subject to a weak viscous damping. The three inherent lengths of the model, defining the multiple-well substrate geometry and the natural equilibrium separation among the chain particles, were chosen to be mutually *commensurate*. Due to this rational choice, and to the imposed periodic boundary conditions for finite size systems, we were able to observe the formation of commensurate dynamical structures during the

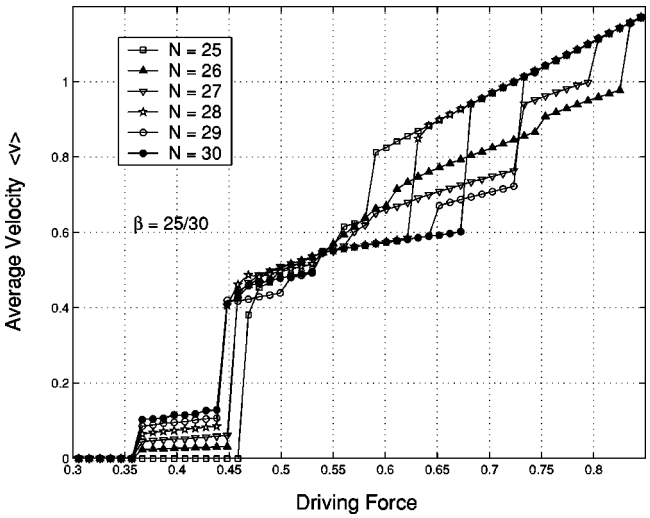

FIG. 9. Average mean velocity vs driving for a chain with different numbers N of particles; $\beta=25/30$.

sliding over the substrate. When these moving structures were extended enough with respect to the substrate period *T*, their topological shape turned out to be decorated by superimposed smaller deformable particle configurations with periodicity *T*. The structure geometries and amplitudes are, clearly, dependent also on the stiffness (i.e., the interatomic strength *K*) and length (i.e., the particle number *N*) of the chain. These dynamical entities characterize the different spatially inhomogeneous stable states, giving rise to the multiple steps found in the chain mobility as a function of the imposed driving force.

Applying an external field *F* to a *multiple-well* substrate leads to a *sequential* disappearance of the substrate potential minima until the situation with no stable particle positions is reached. Varying the number of chain particles allowed us to illustrate the role played by the coverage variable in the depinning mechanism and the difference, in this case, between its static and dynamic commensurability. This characteristic behavior is particularly emphasized when the substrate geometry has maxima and minima with large differences in heights. This may well occur in the real physical situation of lattices with a complex unit cell.

Evidently a detailed analysis of the particle dynamics requires a study for every specific complex substrate shape. Nevertheless, our results allowed us to infer some general qualitative behavior connected to the length scale commensurability of the system. The formation of the observed commensurate structures may be relevant to future studies concerning the sliding of one-dimensional chains over truly irregular (i.e., random) substrate potentials, where, depending on the model parameters, these kind of moving entities could emerge as important mesoscopic elements in the rich multiscale spatio-temporal behavior of the full system.

ACKNOWLEDGMENTS

Two of us (A.V. and V.B.) acknowledge the financial support by INFM under the project PRA: ''Nanorub.'' Work at Los Alamos National Laboratory is supported by the U.S. DOE under Contract No. W-7405-ENG-36.

[1] U. Dehlinger, Ann. Phys. (Leipzig) **2**, 749 (1929).

[2] Y.I. Frenkel and T. Kontorova, Phys. Z. Sowjetunion **13**, 1 (1938); J. Phys. (USSR) **1**, 137 (1939).

[3] O.M. Braun and Y.S. Kivshar, Phys. Rep. **306**, 1 (1998), and references therein.

[4] See, e.g., M. Weiss and F.-J. Elmer, Phys. Rev. B **53**, 7539 (1996); M. Weiss and F.-J. Elmer, Z. Phys. B: Condens. Matter **104**, 55 (1997); O.M. Braun, T. Dauxois, M.V. Paliy, and M. Peyrard, Phys. Rev. Lett. **78**, 1295 (1997); O.M. Braun, T. Dauxois, M.V. Paliy, and M. Peyrard, Phys. Rev. E **55**, 3598 (1997).

[5] See, e.g., B.N.J. Persson, *Sliding Friction: Physical Principles and Applications* (Springer-Verlag, Berlin, 1998).

[6] See, e.g., E.D. Smith, M.O. Robbins, and M. Cieplak, Phys. Rev. B **54**, 8252 (1996); M.R. Sorensen, K.W. Jacobsen, and P. Stoltze, *ibid.* **53**, 2101 (1996); J.E. Hammerberg, B.L. Holian, J. Röder, A.R. Bishop, and S.J. Zhou, Physica D **123**, 330 (1998).

[7] S. Aubry, in *Solitons and Condensed Matter Physics*, edited by A. R. Bishop and T. Schneider, Springer Series in Solid State Sciences (Springer-Verlag, Berlin, 1978), Vol. 8, pp. 264–277; S. Aubry, Physica D **7**, 240 (1983); S. Aubry and P.Y. Le Daeron, *ibid.* **8**, 381 (1983).

[8] P.L. Christiansen, A.V. Savin, and A.V. Zolotaryuk, Phys. Rev. B **57**, 13564 (1998).

[9] A. Vanossi, J. Röder, A.R. Bishop, and V. Bortolani, Phys. Rev. E **63**, 017203 (2001).

[10] J. Röder, A.R. Bishop, B.L. Holian, J.E. Hammerberg, and R.P. Mikulla, Physica D **142**, 306 (2000).

[11] J. Röder, J.E. Hammerberg, B.L. Holian, and A.R. Bishop, Phys. Rev. B **57**, 2759 (1998).

[12] T.S. van Erp *et al.*, Phys. Rev. B **60**, 6522 (1999).

[13] J.S. Ko *et al.*, Surf. Sci. **423**, 245 (1999); L.M. Zhang *et al.*, Wear **229**, 784 (1999).

[14] A. Janner and T. Janssen, Phys. Rev. B **15**, 643 (1977).